International Journal of Pressure Vessels and Piping 203 (2023) 104928

Contents lists available at ScienceDirect

International Journal of Pressure Vessels and Piping

journal homepage: www.elsevier.com/locate/ijpvp

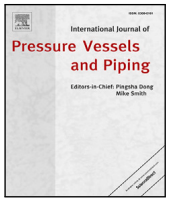

Limit and shakedown analysis of double-layer tube considering different material properties

Jiajiang Du [a], Jin Zhang [a,*], Yanhui Liu [b], Chong Shi [a], Xiusong Shi [a]

[a] Key Laboratory of Ministry of Education for Geomechanics and Embankment Engineering, Hohai University, Nanjing 210024, China
[b] Yellow River Engineering Consulting Co.,Ltd., Zhengzhou 450003, China

ARTICLE INFO

Keywords:
Double-layer tube
Shakedown
Limit analysis
von Mises
Bearing capacity

ABSTRACT

This paper is devoted to the maximum bearing capacity of double-layer tubes subjected to monotonic and cyclic loading, within the framework of static limit and shakedown analysis. The double-layer tube comprises inner and outer layers made of different materials, both obeying the von Mises criterion. The effects of different geometric dimensions (thickness and volume fraction) and material properties (elastic modulus, Poisson's ratio, and yield stress) on the effective mechanical behavior are studied analytically and numerically. The results indicate that the bearing capacity of the double-layer tube under monotonic load reaches its maximum value when both inner and outer layers reach their elastic or plastic limits simultaneously. The computation of plastic and shakedown limits are presented, divided into different cases by considering the volume fraction of the inner and outer layers. The double-layer structure under cyclic loads may fail due to fatigue and excessive deformation mechanisms of the inner or outer layers at the first cycle. Only when both layers fail due to fatigue simultaneously, the shakedown limit of the structure reaches its maximum value. Compared to a single-layer tube, the long-term strength of the double-layer tube can be significantly improved by applying appropriate geometric dimensions and materials in fabrication.

1. Introduction

Single-layer tube is one of the typical structures in engineering, which is used in subterranean pipelines, pressure vessels and helically reinforced tubular structures. It is extensively utilized in chemical manufacturing, mechanical engineering and other industries [1–3]. In order to improve the load bearing capacity of single-layer tube, many researchers select to increase the wall thickness or use higher strength materials. However, simply increasing the wall thickness and employing higher strength materials are not conducive to saving production metals and controlling costs [4–6]. Moreover, the load bearing capacity will not be significantly improved with the continuously increase of the outer radius, if the inner radius of the single-layer tube remains constant [7,8].

Therefore, one of the efficient ways to enhance the load bearing capacity is to apply double-layer structures, in which the stresses will be redistributed and different with those in single-layer tube [9–11], leading to the improvement of performance. A double-layer tube is fabricated by assembling two single-layer tubes together. When the double-layer tube structure is adopted, the inner layer can be made of precious metal materials with high strength and corrosion resistance, while the outer layer can be made of ordinary metal materials with sufficient strength and toughness [12–14]. The material with high yield strength can also be used as the inner layer of the double-layer tube, which can improve its load bearing capacity. Limit analysis and shakedown problems of tubes have been extensively studied in the literature, with most research focused on single-layer ones. However, research on the limit and shakedown analysis of double-layer tubes is not commonly considered, especially the influence of the geometric dimensions and mechanical constants of the double-layer tube on the plastic and shakedown limit [15–17]. This can lead to significant deviations when applied to engineering structures. Moreover, researches [18,19] has shown that spherical shells or cylindrical structures under cyclic loading can fail of fatigue or incremental collapse at the first cycle due to different mechanisms. Therefore, more efforts are needed to study the failure mechanism of double-layer tubes in various conditions.

In recent years, the advantages of double-layered structures have been studied by researchers. Yavari et al. [20] discovered that the presence of eigentwist in a solid can significantly impact a structure's reaction to loads. These effects are related to the nonlinear response of the material, the geometry of the structure, and a variety of eigenstrains, and can be extremely non-trivial in finite deformations. Recent

* Corresponding author.
E-mail address: chelseazhangjin@163.com (J. Zhang).

https://doi.org/10.1016/j.ijpvp.2023.104928
Received 18 January 2023; Received in revised form 18 February 2023; Accepted 1 March 2023
Available online 2 March 2023

Nomenclature

Parameters of single-layer tube

b	Outer radius
ν	Poisson's ratio
k	Volume fraction
σ_θ	Tangential stress
ε_θ	Tangential strain
$\boldsymbol{\sigma}^P$	Stress field in the plastic region

Parameters of double-layer tube

r_b	Middle radius
E_1	Elastic modulus of inner layer
ν_1	Poisson's ratio of inner layer
k_1	Volume fraction of inner layer
α	Ratio of yield stress
$\boldsymbol{\sigma}_1^E$	Stress field in the elastic region of inner layer
δ_1	Displacement at contact position of inner layer
q_1	Contact pressure increment
q	Total contact pressure
$\max p_e$	Maximum value of elastic limit
r_o	Elastoplastic radius of outer layer
p_{p2}	Plastic limit due to outer failure
p_{sd1}	Shakedown limit of inner failure
p_{sd3}	Shakedown limit of simultaneous failure
a	Inner radius
E	Elastic modulus
σ_s	Yield strength
σ_r	Radial stress
ε_r	Radial strain
$\boldsymbol{\sigma}^E$	Stress field in the elastic region
r_a	Inner radius
r_c	Outer radius
E_2	Elastic modulus of outer layer
ν_2	Poisson's ratio of outer layer
k_2	Volume fraction of outer layer
β	Ratio of elastic modulus
$\boldsymbol{\sigma}_2^P$	Stress field in the plastic region of outer layer
δ_2	Displacement at contact position of outer layer
q_0	Contact pressure
p_e	Elastic limit
r_i	Elastoplastic radius of inner layer
p_{p1}	Plastic limit due to inner failure
p_{p3}	Plastic limit due to simultaneous failure
p_{sd2}	Shakedown limit of outer failure

studies [21,22] have demonstrated that a double-layer tube made of two isotropic layers that are twisted in opposing directions and soldered together can achieve the same result by taking advantage of geometrical and material incompatibilities. While the origins of these occurrences in anisotropic tubes are well known, the causes of this effect in isotropic double-layer tubes are less well understood. Researches has shown that combining geometrical dimensions and material properties can demonstrate the inversion and perversion effects. Furthermore, by carefully selecting the material and geometric characteristics in the inner and outer layers, twist behavior may be designed [23,24].

For the determination of load bearing capacity, let us introduce the limit analysis theory, which allows to predict the ultimate load. This theory, developed intuitively in the 1930s, is now widely used and has become recommended by design codes on pressure vessels and on reinforced concrete slabs. Using limit analysis method to calculate the ultimate bearing capacity of the structure does not involve the loading process, which can overcome the difficulties encountered in the calculation of gradual loading. It is an essential method to deal with the maximum strength problem of complex structures [25,26]. On the other hand, as the applicable structures of pressure vessels and gas pipelines, double-layer tube is often exposed to simultaneous variable actions of loads. In the case of variable repeated loads, the magnitude of ultimate load in monotonic case is not the only factor characterizing the structural safety. The experimental tests show that, in some cases, we can observe after a transient phase an accumulation of plastic strains leading to excessive deformations and reversed plastic deformations [27]. These two kind of failure is called incremental collapse (ratcheting) and accommodation (fatigue) [28,29]. The structural safety requires that the power dissipated by the plastic deformation due to repeated load should eventually cease, where the cyclic behaviors will eventually become pure elastic responses [19,30]. The corresponding safety load is called shakedown limit load, below which the structural safety is guaranteed. This indicates to introduce the shakedown analysis theories [31,32], developed from limit analysis, which does not require the complex loading history and leads to the simplicity of computation [33,34]. In particular, the collapse by development of a mechanism, as in limit analysis, can be observed as the special case of ratcheting during the first cycle in cyclic loading case if the load magnitude is too large. This will lead to different fracture mechanism of the considered tube structures.

Currently, the available studies of double-layer tube are mainly focused on the same material of inner and outer layers, which greatly reduces the flexibility of structure design. Consequently, we aim at calculating the ultimate strength of double layer tube under monotonic load and long-term strength under cyclic loads by limit and shakedown analysis methods, respectively. The effects of different material properties and geometric designs will be considered. Firstly, we examine the stress and displacement condition of the inner and outer layers by using various materials, and provide the analytical solution for elastic limit. Then, the plastic limit is discussed in three cases. It is discussed through the classification of the volume fraction of the inner and outer layers, and it can be divided into four cases where the inner and outer layers will fail due to different failure mechanism (incremental collapse and fatigue). This paper proposes an analytical approach to determine the optimum geometric design of the double-layer tube by considering various material properties. The analytical derivation of the optimal geometric design is of great importance for engineering applications. The displacement continuity equation at the contact position is derived, and the conditions for the inner and outer layers to reach the elastic and shakedown limit simultaneously are obtained. This advancement will significantly improve the elastic and shakedown limit of the double-layer tube compared to the single-layer one, making it a more efficient in engineering applications. It is found that when the inner and outer layers simultaneously reach the elastic and shakedown limit, the ultimate bearing capacity of double-layer tube will be significantly improved [35–37]. The plastic failure modes of the double-layer tube are discussed in detail, and we derive the analytical conditions for judging the plastic failure modes based on geometric size and mechanical properties. We identify three types of plastic failure in the double-layer tube and find that adjusting the geometric dimensions and material properties can lead to different failure modes. By comparing the shakedown and plastic limits of the single-layer tube, we find that the different failure modes of the double-layer cylinder is related to the volume fraction k of the inner and outer layers.

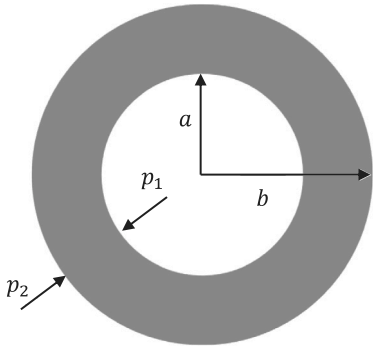

Fig. 1. The cross section of single-layer tube.

Four failure modes based on volume fraction k is identified and the analytical value of the limit stress for each mode is computed. It is also found that only when both layers fail due to fatigue simultaneously, the shakedown limit of the double-layer tube reaches its maximum value.

This paper is organized in the following order. The problem description and basic formations is provided in Section 2. We start from the simplest case of singer-layer tube, and then extend to double layer case. The effects of geometric condition and material properties on the elastic limit are determined, as well as the relationship between the internal pressure load and the contact pressure. In Section 3, by the use of the displacement continuity condition at the contact surface, the plastic failure in monotonic load case of the double-layer tube is obtained. It is found that the plastic limit of the double-layer tube reaches the maximum when both the inner and outer layers reach the complete plastic state. Then, according to different the volume fraction of the inner and outer layers subjected to cyclic loads, the fatigue failure and excessive deformation in the first cycle are divided into four cases in Section 4 in view of shakedown analysis. The shakedown limit load of the double-layer tube is also computed developed from the single layer case. The last section is devoted to the conclusions.

2. Problem description and basic formulations

In this study, we aim at providing the plastic limit and shakedown limit of double-layer tube considering the different materials properties of inner and outer layers. To start from the simplest case, the basic formulations and computation of elastic limit of single layer tube will be firstly provided in the first subsection, and then extended to the double-layer case in the second and third subsections.

2.1. Plastic and shakedown limit of single-layer tube

We consider the stress and displacement fields in the hollow tube described by cylindrical coordinate $\{\mathbf{e}_r, \mathbf{e}_\theta, \mathbf{e}_z\}$. Since the single-layer tube is axisymmetric, the stress and displacement are only single-valued functions of radius r. In this paper, von Mises yield criterion is adopted and the material is considered to be elastic perfectly-plastic, as shown in Fig. 1. The inner and outer radii are respectively denoted a and b, giving the void volume fraction $k = a^2/b^2 < 1$. The single-layer tube is subjected to a uniform stress p_1 and p_2 upon its inner and outer boundaries.

The differential equation of stress equilibrium condition for the considered structure can be written as:

$$\frac{d\sigma_r}{dr} + \frac{\sigma_r - \sigma_\theta}{r} = 0 \tag{1}$$

where σ_r is the radial stress and σ_θ is the tangential stress.

Considering axial symmetry of single-layer tube, its geometric equation takes the form as:

$$\varepsilon_r = \frac{du}{dr}, \quad \varepsilon_\theta = \frac{u}{r} \tag{2}$$

where ε_r is the radial strain and ε_θ is the tangential strain.

The elastic constitutive equation of the tube reads:

$$\begin{cases} \varepsilon_r = \dfrac{1}{E}(\sigma_r - \nu\sigma_\theta) \\ \varepsilon_\theta = \dfrac{1}{E}(\sigma_\theta - \nu\sigma_r) \end{cases} \tag{3}$$

where E and ν represent Young's modulus and Poisson's ratio, respectively.

Since the inner and outer surfaces are subjected to internal outer pressures p_1 and p_2, the boundary conditions can be obtained as:

$$\sigma_r(a) = p_1, \quad \sigma_r(b) = p_2 \tag{4}$$

By combining Eqs. (1), (2), (3) and (4), the elastic stress field of single-layer tube can be provided in the cylindrical frame:

$$\boldsymbol{\sigma}^E = \left(\frac{p_2 - p_1}{1-k}\right)\frac{a}{r^2}(\boldsymbol{e}_r\otimes\boldsymbol{e}_r - \boldsymbol{e}_\theta\otimes\boldsymbol{e}_\theta) + \frac{kp_1 - p_2}{1-k}(\boldsymbol{e}_r\otimes\boldsymbol{e}_r + \boldsymbol{e}_\theta\otimes\boldsymbol{e}_\theta + \frac{1}{2}\boldsymbol{e}_z\otimes\boldsymbol{e}_z) \tag{5}$$

the introduced volume fraction parameter is defined as $k = a^2/b^2$ in the equation.

Similarly, one has the elastic displacement field:

$$u = \frac{(1+\nu)(p_1 - p_2)a^2}{E(1-k)r} + \frac{(1-\nu)(kp_1 - p_2)r}{E(1-k)} \tag{6}$$

Adopting the von Mises yield criterion, the single-layer tube is made of an elasto-plastic material obeying the following function:

$$F(\boldsymbol{\sigma}) = \sigma_{eq}(\boldsymbol{\sigma}) - \sigma_s \le 0 \tag{7}$$

where $\sigma_{eq} = \sqrt{\frac{3}{2}\boldsymbol{s} : \boldsymbol{s}}$ is the equivalent stress defined from the deviatoric part $\boldsymbol{s}$ of the stress tensor $\boldsymbol{\sigma}$. $\sigma_s > 0$ represents the yield stress. The plastic strain rate tensor is given by the normality law:

$$\dot{\boldsymbol{\varepsilon}}^p = \lambda\frac{\partial F}{\partial \boldsymbol{\sigma}} \tag{8}$$

where $\lambda \ge 0$ is the plastic multiplier.

On the other hand, the elastic strains are related to the stresses by Hookes law:

$$\boldsymbol{\varepsilon}^e = \boldsymbol{D} : \boldsymbol{\sigma} \tag{9}$$

where $\boldsymbol{D}$ is the compliance tensor.

The total strain $\boldsymbol{\varepsilon}$ can be divided into elastic and plastic parts, combining the properties of elasticity and plasticity:

$$\boldsymbol{\varepsilon} = \boldsymbol{\varepsilon}^e + \boldsymbol{\varepsilon}^p \tag{10}$$

Considering Eqs. (5) and (7), the yield function condition of the single-layer tube can be computed by:

$$\max_{r_a \le r \le r_b}\sigma_{eq} = \max_{r_a \le r \le r_b}\sqrt{3}\left(\frac{p_1 - p_2}{1-k}\right)\frac{a^2}{r^2} \le \sigma_s \tag{11}$$

As a result, the elastic limit can be obtained by considering the initial yielding condition at inner boundary $r = a$:

$$p_1 - p_2 = \frac{1}{\sqrt{3}}\sigma_s(1-k) \tag{12}$$

Taking Eqs. (1), (4) and (7) into account, the stress field in plastic region is:

$$\boldsymbol{\sigma}^P = \left(\frac{2\sigma_s}{\sqrt{3}}\ln\left(\frac{r}{a}\right) - p_1\right)(\boldsymbol{e}_r\otimes\boldsymbol{e}_r + \boldsymbol{e}_\theta\otimes\boldsymbol{e}_\theta + \boldsymbol{e}_z\otimes\boldsymbol{e}_z) + \frac{2\sigma_s}{\sqrt{3}}(\boldsymbol{e}_\theta\otimes\boldsymbol{e}_\theta + \frac{1}{2}\boldsymbol{e}_z\otimes\boldsymbol{e}_z) \tag{13}$$

If the whole section of tube is filled with plastic zone $F(\boldsymbol{\sigma})_{r=b} = 0$, the plastic limit of single-layer tube is:

$$p_1 - p_2 = -\frac{1}{\sqrt{3}}\sigma_s \ln k \tag{14}$$

Beyond this elastic limit, plastic strains appear. For the variable loading case, if the tube shakes down the applied loads p_1 and p_2 belong to the domain:

$$(p_1-p_2)_- \le p_1-p_2 \le (p_1-p_2)_+ = (p_1-p_2)_- + \Delta(p_1-p_2) \tag{15}$$

where $(p_1-p_2)_\pm$ denote the maximum and minimum values of (p_1-p_2).

For the application of Melan's theorem [31], the critical idea of the statical approach is to determine the admissible residual stress fields $\bar{\rho}$ according to De Saxcé [18]:

- $\bar{\rho}$ is time-independent,
- $\bar{\rho}$ is a residual stress field,
- $\bar{\rho}$ is strictly plastically admissible in the sense that $F(\sigma^E+\bar{\rho})<0$ at any time.

Because of the axial symmetry, the residual stress field is assumed in the following form:

$$\bar{\rho} = \bar{\rho}_{rr}\boldsymbol{e}_r\otimes\boldsymbol{e}_r + \bar{\rho}_{\theta\theta}\boldsymbol{e}_\theta\otimes\boldsymbol{e}_\theta + \bar{\rho}_{zz}\boldsymbol{e}_z\otimes\boldsymbol{e}_z \tag{16}$$

and must satisfy the only internal equilibrium equation:

$$r\frac{d\bar{\rho}_{rr}}{dr} = \bar{\rho}_{\theta\theta} - \bar{\rho}_{rr} \tag{17}$$

In order to construct the residual stress field, it is inspired from the statical solution of hollow tube only subjected to outer pressure [18]:

$$\left| r\frac{d\bar{\rho}_{rr}}{dr} + \sqrt{3}\left(\frac{p_1-p_2}{1-k}\right)\frac{a^2}{r^2}\right| \le \sigma_s \tag{18}$$

The previous inequality is satisfied for the specified load domain provided that:

$$\begin{aligned} -\sigma_s &\le r\frac{d\bar{\rho}_{rr}}{dr} + \sqrt{3}\left(\frac{p_1-p_2}{1-k}\right)_-\frac{a^2}{r^2} \le \sigma_s,\\ -\sigma_s &\le r\frac{d\bar{\rho}_{rr}}{dr} + \sqrt{3}\left(\frac{p_1-p_2}{1-k}\right)_+\frac{a^2}{r^2} \le \sigma_s \end{aligned} \tag{19}$$

We only keep the strongest inequalities while taking into account the superior and inferior envelopes:

$$-\sigma_s - \sqrt{3}\left(\frac{p_1-p_2}{1-k}\right)_-\frac{a^2}{r^2} \le r\frac{d\bar{\rho}_{rr}}{dr} \le \sigma_s - \sqrt{3}\left(\frac{p_1-p_2}{1-k}\right)_+ \tag{20}$$

Therefore, there exists a time-independent residual stress field only if for $a \le r \le b$:

$$\Delta(p_1-p_2)\frac{a^2}{r^2} = \frac{2}{\sqrt{3}}\sigma_s(1-k) \tag{21}$$

If the pressure $(p_1-p_2)_- = 0$, we can get the shakedown limit of the single-layer tube as:

$$p_1-p_2 = \frac{2}{\sqrt{3}}\sigma_s(1-k) \tag{22}$$

2.2. Double-layer tube with contact pressure increment at intermediate surface

The materials that make up the inner and outer layers are diverse, and so are their mechanical characteristics and geometric dimensions. In order to assemble the outer layer on the inner layer, the outer layer is usually heated to make its geometric size larger. Therefore, the outer layer can then be assembled on the inner layer, which forms a double-layer tube. After the assembly is completed, the temperature of the outer layer will gradually decrease and its geometric size will shrink. Then, it will produce a uniform interaction force between the intermediate surface of the inner and outer layer, which will be noted as the contact pressure q_0.

After assembly, the inner and outer layers combine to produce a double-layer tube, which is illustrated in Fig. 2. The inner and outer radii are noted as r_a and r_c, and the radius of intermediate surface is r_b. If the internal pressure p is applied to it, there will be a contact pressure increment q_1 at the contact position and there is a single-valued relationship between them. q_1 is not a real external pressure, but an internal pressure that depends on the applied load p. In this study, q_0 at the contact surface due to the heating of the outer layer is defined as the initial contact pressure. Since q_1 is also at the contact surface, the total applied load at the outer wall q is the sum of the contact pressure q_0 and q_1 ($q = q_0 + q_1$) by isolating the inner layer (see Fig. 2(a)). Therefore, the functional relationship between q_1 and p can be derived by the displacement continuity condition at the contact position. With the increase of internal pressure, the contact pressure increment will also increase. Ignoring the initial contact pressure q_0, the isolated inner layer is not only affected by the internal pressure p, but also by q_1, while the isolated outer layer is only subjected to q_1.

Using the result of single-layer case (5), we obtain the elastic stress field of inner layer:

$$\boldsymbol{\sigma}_1^E = \left(\frac{q_1-p}{1-k_1}\right)\frac{r_a^2}{r^2}(\boldsymbol{e}_r\otimes\boldsymbol{e}_r - \boldsymbol{e}_\theta\otimes\boldsymbol{e}_\theta) + \frac{k_1p-q_1}{1-k_1}(\boldsymbol{e}_r\otimes\boldsymbol{e}_r + \boldsymbol{e}_\theta\otimes\boldsymbol{e}_\theta + \frac{1}{2}\boldsymbol{e}_z\otimes\boldsymbol{e}_z) \tag{23}$$

where E_1, ν_1 and $k_1 = r_a^2/r_b^2$ are Young's modulus, Poisson's ratio and volume fraction of the inner layer, respectively.

Similarly, displacement field of inner layer can be written as:

$$u_1 = \frac{(1+\nu_1)(p-q_1)r_a^2}{E_1(1-k_1)r} + \frac{(1-\nu_1)(k_1p-q_1)r}{E_1(1-k_1)} \tag{24}$$

The stress field of outer layer takes the form as:

$$\boldsymbol{\sigma}_2^E = \frac{k_2q_1}{1-k_2}(\boldsymbol{e}_r\otimes\boldsymbol{e}_r + \boldsymbol{e}_\theta\otimes\boldsymbol{e}_\theta + \boldsymbol{e}_z\otimes\boldsymbol{e}_z) + \left(\frac{q_1}{1-k_2}\right)\frac{r_b^2}{r^2}(-\boldsymbol{e}_r\otimes\boldsymbol{e}_r + \boldsymbol{e}_\theta\otimes\boldsymbol{e}_\theta) \tag{25}$$

where E_2, ν_2 and $k_2 = r_b^2/r_c^2$ are Young's modulus and Poisson's ratio and volume fraction of the outer layer.

The displacement field of outer layer can be computed as:

$$u_2 = \frac{(1+\nu_2)q_1r_b^2}{E_2(1-k_2)r} + \frac{(1-\nu_2)k_2q_1r}{E_2(1-k_2)} \tag{26}$$

Let us introduce a coefficient μ_1, where the relationship between p and q_1 can be defined as $p = \mu_1 q_1$. By integrating Eqs. (24), (26) and $u_1(b) = u_2(b)$, we can obtain the expression of μ_1:

$$2\mu_1 = 1+\nu_1+(1-\nu_1)k_1^{-1} + \beta k_1^{-1}(1-k_1)(1-k_2)^{-1}[1+\nu_2+(1-\nu_2)k_2] \tag{27}$$

Fig. 3 illustrates the variation of the introduced coefficient μ_1^{-1} in different geometric dimensions with respect to the different value of β (ratio of Young's moduli between inner and outer layers). We can find that as the thickness of inner layer increases, the value of μ_1^{-1} also increases (Fig. 3(a)). If the thickness of the outer layer becomes larger, the coefficient μ_1^{-1} will become smaller (Fig. 3(b)). The coefficient μ_1 will change with respect to the elastic modulus ratio, and the greater the elastic modulus ratio is, the greater the coefficient μ_1 will be. When the thickness of the inner cylinder is zero, the structure will be reduced to a single-layer tube, and the value of the coefficient μ_1 is 1, which is also in good agreement with the actual situation.

2.3. Elastic limit of double-layer tube

Now we consider the contact pressure q_0. The contact pressure q_0 is due to the assembly of the double-layer tube. Specifically, during the fabrication process, the outer layer is heated to expand its geometrical dimension, and then it is assembled onto the inner layer. As the outer layer cools down, its radius will shrink, generating contact pressure q_0 at the contact position of the double-layer tube. As a result, the inner layer is subjected to contact pressure q_0 in the outer wall, and the outer layer is subjected to contact pressure q_0 in the inner wall. Based on the displacement equation Eq. (6) of the single-layer tube,

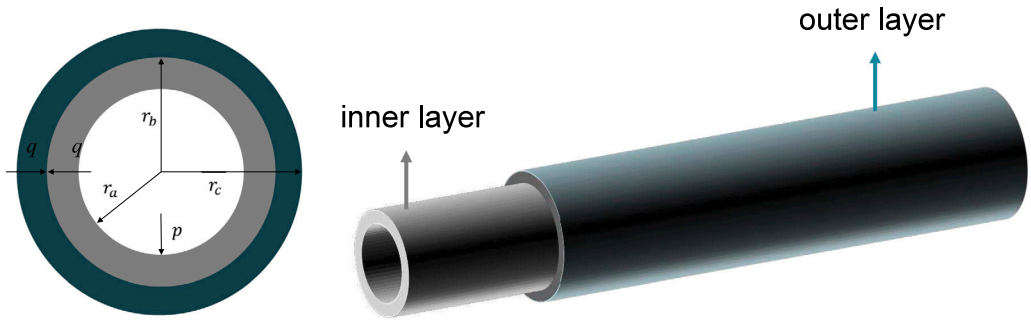

(a) The front section (b) The side view

Fig. 2. The cross section and side view of double-layer tube composed of different materials.

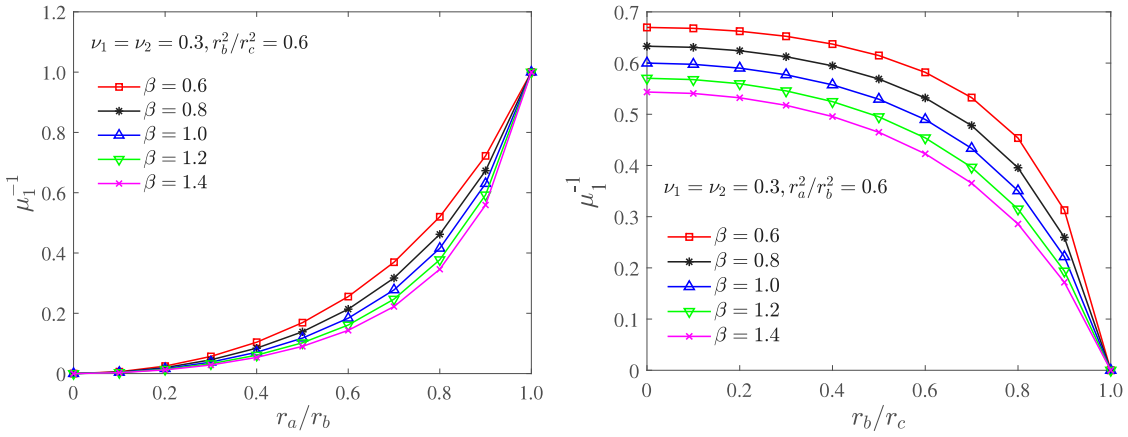

(a) Curves of $\mu_1^{-1} - r_a/r_b$ under different β (b) Curves of $\mu_1^{-1} - r_b/r_c$ under different β

Fig. 3. Variation of μ_1 with respect to different values of $\beta = E_1/E_2$.

we can derive the displacements of the inner and outer layers (δ_1 and δ_2) under contact pressure q_0:

$$\delta_1 = u(r_b)|_{p_1=0,p_2=q_0} = \frac{[(1+\nu_1)k_1 + 1 - \nu_1]r_b q_0}{E_1(1-k_1)} \tag{28}$$

and

$$\delta_2 = u(r_b)|_{p_1=q_0,p_2=0} = \frac{[(1-\nu_2)k_2 + 1 + \nu_2]r_b q_0}{E_2(1-k_2)} \tag{29}$$

Combining $\delta = \delta_1 + \delta_2$ with the above equation, we can obtain that:

$$q_0 = \mu_0 \delta \tag{30}$$

where

$$\mu_0 = r_b^{-1}\left[\frac{(1+\nu_1)k_1 + 1 - \nu_1}{E_1(1-k_1)} + \frac{(1-\nu_2)k_2 + 1 + \nu_2}{E_2(1-k_2)}\right]^{-1} \tag{31}$$

If the contact pressure q_0 is calculated using the original dimensions ($r_b + \delta_1$ and $r_b - \delta_2$), the expression for the volume fraction $k_1 = r_a^2/r_b^2$ will need to be changed to a more complex form $k_1 = r_a^2/(r_b+\delta_1)^2$. This will increase the equation complexity and the amount of computation required. However, since δ_1 is much smaller than r_b, the volume fraction expression k1 shows that the volume fraction before and after deformation is approximately equal ($r_b^2 \approx (r_b+\delta_1)^2$). Therefore, using the deformed diameter (r_b) to calculate the contact pressure will result in minimal deviation and greatly simplify the complexity of expressions.

The variations of $r_b\mu_0/E_1$ in different geometric dimensions with respect to the different value of β are provided in Fig. 4. When the inner and outer layers thickness increases, the coefficient μ_0 will gradually decreases. For the particular case where the inner or outer layer thickness is reduced to zero (r_a/r_b or $r_b/r_c = 1$), the value of the coefficient μ_0 will be reduced to zero. The value of the coefficient μ_0 becomes smaller with the decrease of the elastic modulus ratio β.

The inner and outer layers of the tube are expected to be in the elastic limit state simultaneously, which provide us the following conditions:

$$\frac{2(p-q)}{1-k_1} = \frac{2}{\sqrt{3}}\sigma_{s1}, \quad \frac{2q}{1-k_2} = \frac{2}{\sqrt{3}}\sigma_{s2} \tag{32}$$

where σ_{s1} and σ_{s2} is the yield stresses of inner and outer layers.

If both the inner and outer layers simultaneously approach their elastic limit, there will exist a certain relationship between p and q, which is noted as $p = \mu q$. Taking Eq. (32) into account, the expression of coefficient μ can be stated as follows:

$$\mu = (1-k_2)^{-1}[1 - k_2 + \alpha(1-k_1)] \tag{33}$$

where $\alpha = \sigma_{s1}/\sigma_{s2}$ is the ratio of yield stresses between inter and outer layers.

Hence, a suitable difference between outer radius of inner layer and inner radius of outer layer before assembly can be found (noted as δ) of double-layer tube. In practical engineering applications, the inner and outer layer will reach the elastic limit at the same time if the δ satisfies Eq. (34). By combining $p = \mu_1 q_1$, $q_0 = \mu_0\delta$, $p = \mu q$, and $q = q_0 + q_1$, the expression of parameter δ can be derived as:

$$\delta = \mu_0^{-1}(\mu^{-1} - \mu_1^{-1})p \tag{34}$$

Now we consider a double-layer tube satisfying the above condition. Using Eq. (32), the elastic limit of the double-layer tube can be given by:

$$p_e = \frac{1}{\sqrt{3}}\sigma_{s2}[1 - k_2 + \alpha(1-k_1)] \tag{35}$$

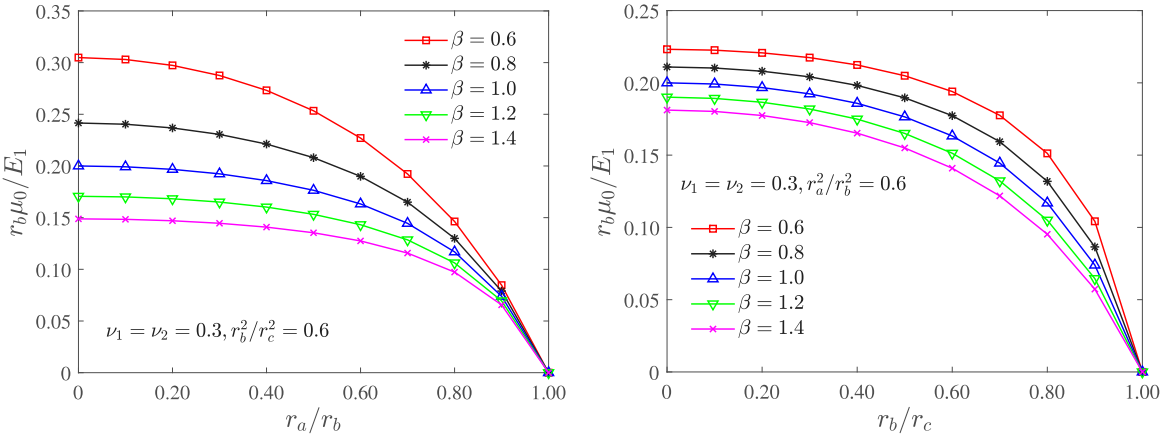

(a) Curves of $r_b\mu_0/E_1 - r_a/r_b$ under different β (b) Curves of $r_b\mu_0/E_1 - r_b/r_c$ under different β

Fig. 4. Variation of $r_b\mu_0/E_1$ with respect to different values of $\beta = E_1/E_2$.

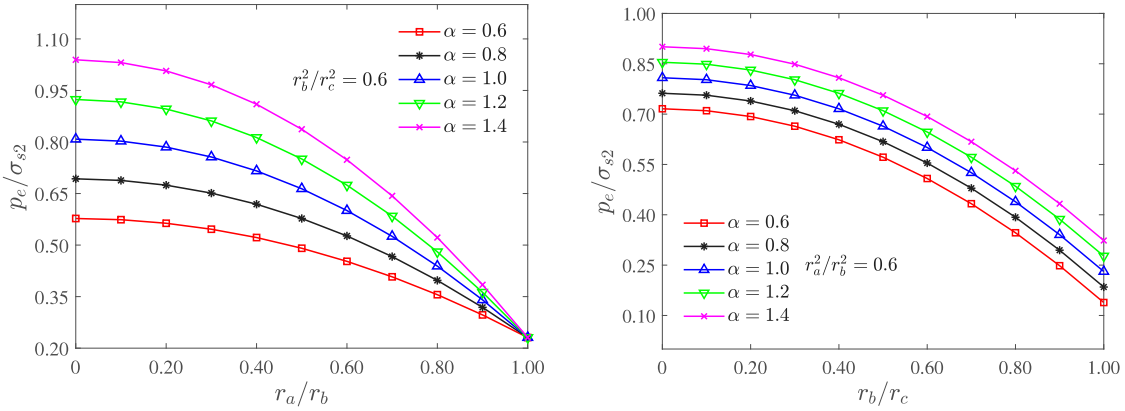

(a) Curves of $p_e/\sigma_{s2} - r_a/r_b$ under different α (b) Curves of $p_e/\sigma_{s2} - r_b/r_c$ under different α

Fig. 5. Variation of p_e with respect to different values of $\alpha = \sigma_{s1}/\sigma_{s2}$.

Using the derivative relationship $\partial p_e/\partial r_b = 0$, it can be obtained that p_e can take the maximum value $\max p_s$ when $r_b = \sqrt{\alpha r_a r_c}$. The expression of the maximum elastic limit $\max p_e$ is:

$$\max p_e = \frac{1}{\sqrt{3}}\sigma_{s2}(\alpha+1)(r_c - r_a)(r_c - \alpha r_a)^{-1}(1 - k_2^{-1}) \tag{36}$$

The elastic limit p_e of double-layer tube is related to σ_{s1}, σ_{s2}, $k_1 = r_a^2/r_b^2$ and $k_2 = r_b^2/r_c^2$. The variation of p_e is shown in Fig. 5 by considering different geometric dimensions of inner and outer layers. In order to investigate the effects of parameter α on the elastic limit p_e, the value of α is set to be 0.6, 0.8, 1.0, 1.2 and 1.4. It can be concluded that the elastic limit p_e increases with the stress ratio parameter α. However, as the thickness reduces, the elastic limit also decreases both in two cases of Fig. 5.

Now we compare the elastic limit p_e of single-layer tube and double-layer tube having the same thickness. Fig. 6 illustrates the difference in elastic limit between them. A significant improvement of elastic limit can be observed for the double-layer tube. If the yield stress of the double-layer tube is reduced by 40%, then the same load bearing capacity can also be achieved by increasing the thickness. However, in engineering application, the thickness cannot be increased infinitely. Under the condition of constant thickness, we can improve the elastic limit by controlling the middle radius r_b as shown in Fig. 6.

3. Plastic limit of double-layer tube under monotonic load

With the continuous increase of the internal pressure p, the inner and outer layers will be in elastoplastic state. It is known that the inner or outer layer will enter into the plastic state from the inner part, and the plastic zone will develop further outward the outer boundary with the increase of p. If the plastic zone fills the entire section, then it can be considered that the inner or outer layers has reached a complete plastic state, in other words, it has undergone plastic failure.

For the double-layer tube, the behavior of plastic failure is more complicated than the single-layer tube. The plastic failure can be divided into three types: the plastic failure of inner layer; the plastic failure of outer layer; the inner and outer layers are in a completely plastic limit state at the same time. They will be fully discussed in this section.

3.1. Displacement continuity equation

The following part describes elastoplastic radius, stress continuity and displacement continuity conditions, when both the inner and outer layers are in the elastoplastic state. In the transition of the elastic and plastic zone, the continuity conditions always need to be fulfilled in both inner and outer layers. The displacement continuity condition must be satisfied at the contact surface. As shown in Fig. 7(a), the inner

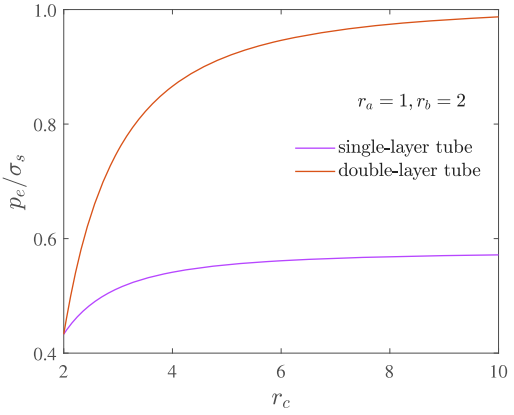

(a) Curves of $p_e/\sigma_s - r_c$ under indentical yield strength between single-layer tube and double-layer tube

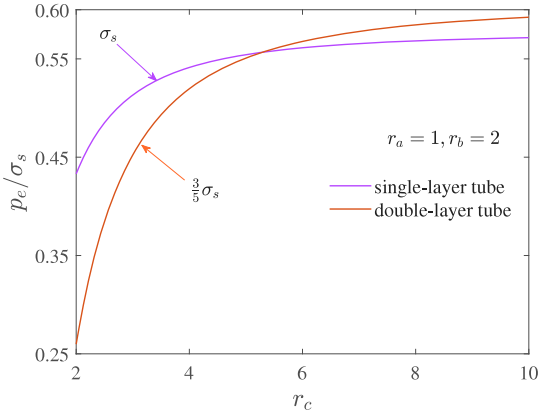

(b) Curves of $p_e/\sigma_s - r_c$ under different yield strength between single-layer tube and double-layer tube

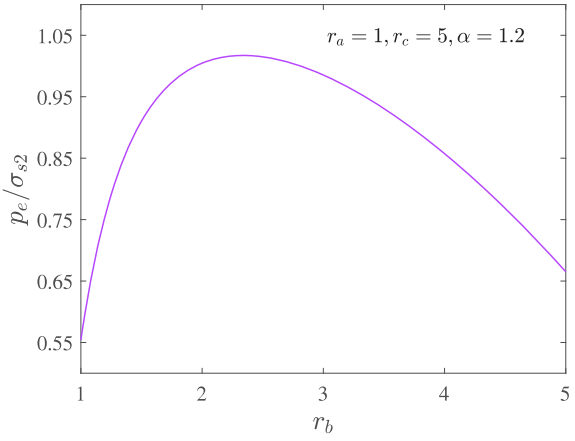

(c) Curve of $p_e/\sigma_{s2} - r_b$ of the double-layer tube

Fig. 6. The comparisons of elastic limit between single-layer tube and double-layer tube.

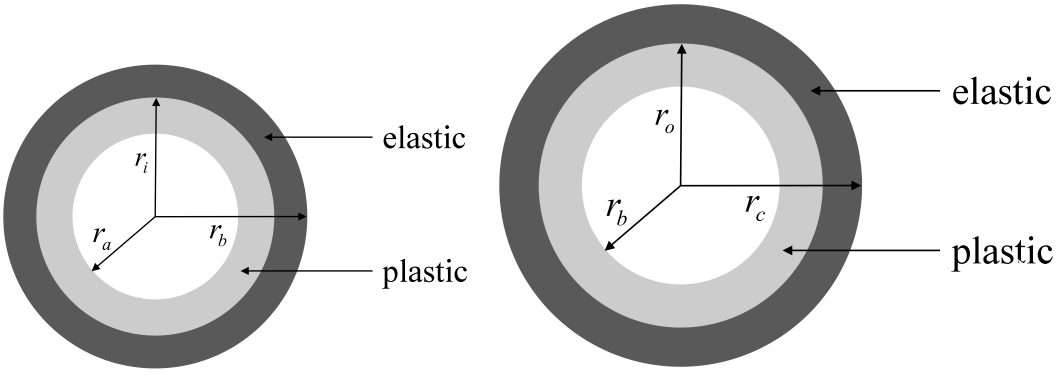

(a) Inner layer (b) Outer layer

Fig. 7. The cross section of double-layer tube in elasto-plastic state.

layer contains an elastic zone $r_i \le r \le r_b$ and a plastic zone $r_a \le r \le r_i$. Similarly, the outer layer is composed of an elastic zone $r_o \le r \le r_c$ and a plastic zone $r_b \le r \le r_o$ (see Fig. 7(b)).

Considering Eq. (5), the radial stress of the inner layer at the elastic region $r = r_i$ can be obtained as:

$$\sigma_r(r_i) = -\frac{1}{\sqrt{3}}\sigma_{s1}\left(1 - \frac{r_i^2}{r_b^2}\right) - q \tag{37}$$

Similarly, the radial stress of the inner layer in the plastic region $r = r_i$ takes the form as:

$$\sigma_r(r_i) = \frac{2}{\sqrt{3}}\sigma_{s1}\ln(r_i/r_a) - p \tag{38}$$

By combining Eqs. (37) and (38), the stress continuity equation is given by:

$$p - q = \frac{1}{\sqrt{3}}\sigma_{s1}\left(1 - \frac{r_i^2}{r_b^2}\right) + \frac{2}{\sqrt{3}}\sigma_{s1}\ln\frac{r_i}{r_a} \tag{39}$$

Similarly, the stress continuity condition of the outer layer can be expressed as:

$$q = \frac{1}{\sqrt{3}}\sigma_{s2}\left(1 - \frac{r_o^2}{r_c^2}\right) + \frac{2}{\sqrt{3}}\sigma_{s2}\ln\frac{r_o}{r_b} \tag{40}$$

Taking Eqs. (24) and (26) into account, the radial displacement in elastic zone of inner layer is obtained as:

$$u_1(r_b) = \frac{\sigma_{s1}r_i^2}{\sqrt{3}E_1 r}[1 + \nu_1 + (1-\nu_1)r_b^{-2}r^2] - \frac{(1-\nu_1)qr}{E_1} \tag{41}$$

And the radial displacement in plastic zone of outer layer is:

$$u_2(r_b) = \frac{\sigma_{s2}r_o^2}{\sqrt{3}E_2 r}[1 + \nu_2 + (1-\nu_2)r_o^2 r_c^{-2}] \tag{42}$$

The displacement continuity condition at contact surface $r = r_b$ can be obtained from Eqs. (41) and (42):

$$2\alpha r_i^2 = \sqrt{3}(1-\nu_1)\sigma_{s2}^{-1}r_b^2 q + \beta r_o^2[1 + \nu_2 + (1-\nu_2)r_o^2 r_c^{-2}] \tag{43}$$

With the above formulations, the plastic failure modes of double-layer tube under monotonic load will be discussed in the following part.

3.2. Plastic failure modes of double-layer tube

There are three plastic failure modes of double-layer tube as mentioned at the beginning of this section. The method for distinguishing the plastic failure of the double-layer tube is discussed as follows: if the inner or outer layer is in elasto-plastic state, the radii r_i or r_o separating the elastic and plastic regions will be used as the index for measuring the degree of load capacity. According to the displacement continuity Eq. (43), we can determine the unique relationship between r_i and r_o as shown in Fig. 7.

3.2.1. Plastic limit due to the failure of inner layer

If the outer layer reaches a completely plastic state, in other words, the elastoplastic radius r_o in outer layer equals r_c, the pressure at the contact surface of the inner and outer layers reads:

$$q = -\frac{1}{\sqrt{3}}\sigma_{s2}\ln k_2 \tag{44}$$

In this situation, the elastoplastic radius of the inner layer r_i can be calculated by the displacement continuous equation. Using Eqs. (40), (43) and (44), the elastoplastic radius of the inner layer can be obtained as follows:

$$r_i = r_c\sqrt{\alpha^{-1}[\beta - \frac{1}{2}(1-\nu_1)k_2\ln k_2]} \tag{45}$$

By comparing the calculated elastoplastic radius r_i by Eq. (45) and r_b, it is possible to judge the first plastic failure between the inner and outer layer. If $r_i > r_b$, it shows that the inner layer has experienced plastic failure earlier than the outer layer. According to Eq. (45), it can be seen that plastic failure of inner layer can also be expressed as:

$$\alpha < \beta k_2^{-1} - \frac{1}{2}(1-\nu_1)\ln k_2 \tag{46}$$

Since the outer layer is in an elastoplastic state in this instance while the inner layer has reached a completely plastic state, the elastic–plastic radius of the inner layer can be known as $r_i = r_b$. By substituting it into Eq. (43), the elastoplastic radius of the inner layer can be determined uniquely as $r_o = \lambda_1 r_c$, where the introduced coefficient λ_1 is a load-independent quantity, related to the mechanical properties and the geometric parameters of the double-layer tube. It can be expressed in the following form:

$$(1-\nu_1)[1 - \lambda_1^2 + \ln(\lambda_1^2 k_2^{-1})] + \beta\lambda_1^2 k_2^{-1}[1 + \nu_2 + (1-\nu_2)\lambda_1^2] - 2\alpha = 0 \tag{47}$$

Following the previous discussion, we know the plastic failure will occur in the inner layer. Therefore, by combining Eqs. (39) and (40), the plastic limit of double-layer tube can be computed:

$$p_{p1} = \frac{1}{\sqrt{3}}\sigma_{s2}[1 - \lambda_1^2 + \ln(\lambda_1^2 k_1^{-\alpha}k_2^{-1})] \tag{48}$$

Due to the symmetry of the double-layer tube, we use a quarter of the structure to reduce the computational effort. The inner layer was meshed using 1200 elements and 1271 nodes, while the outer layer was meshed with 800 elements and 861 nodes. The computation is carried out with the following data: $\alpha = 1.2$, $\beta = 1$, $\nu_1 = \nu_2 = 0.1$, $\sigma_{s1} = 100$, $r_a = 0.4$, $r_b = 0.8$, $r_c = 1$. According to Eq. (48), the limit stress can be computed where the inner layer fails first. Therefore, we can determine the intermediate radius of the inner layer as $r_i = r_b = 0.8$, and then derive the intermediate elastoplastic radius r_o of the outer layer according to the displacement continuity condition Eq. (43). Finally, using the stress continuity condition Eqs. (39) and (40), the values of p and q can be obtained. The equivalent plastic strain (PEEQ) distribution of inner and outer layers under monotonic load are illustrated in Fig. 8. The geometric and elastic parameters are set as $\alpha = 1.2, \beta = 1, \nu_1 = \nu_2 = 0.3$ and $r_b^2/r_c^2 = 0.64$. It can be seen that the entire region of the inner layer will be covered in plastic zones if the inner layer firstly fails due to plastic failure (Fig. 8(a)). At this time, only the region near the inner boundary of the outer layer is in plastic state, while the section near the outer wall is still in elastic state (Fig. 8(b)).

3.2.2. Plastic limit due to the failure of outer layer

In this part, the case of outer layer in completely plastic state will be considered, while the inner layer is in an elastic–plastic state. At this time, the elastoplastic radius of the outer layer satisfies $r_o = r_c$, the elastoplastic radius of the inner layer fulfills $r_i < r_b$. In addition, the plastic failure of the outer layer can also be expressed as follows:

$$\alpha > \beta k_2^{-1} - \frac{1}{2}(1-\nu_1)\ln k_2 \tag{49}$$

As the derivation in the previous part, the elastoplastic radius $r_o = r_c$ of the outer layer and the elastoplastic radius of the corresponding inner layer can be uniquely calculated by the Eq. (43). Hence, the elastoplastic radius of the inner layer is $r_i = \lambda_2 r_b$ and the coefficient λ_2 can be expressed in the following form:

$$(1-\nu_1)k_2\ln(k_2) + 2\alpha\lambda_2^2 k_2 - 2\beta = 0 \tag{50}$$

Taking Eqs. (39) and (40) into account, the plastic limit of the tube due to plastic collapse of outer layer can be expressed as follows:

$$p_{p2} = \frac{1}{\sqrt{3}}\sigma_{s2}[\alpha - \alpha\lambda_2^2 + \ln(\lambda_2^{2\alpha}k_1^{-\alpha}k_2^{-1})] \tag{51}$$

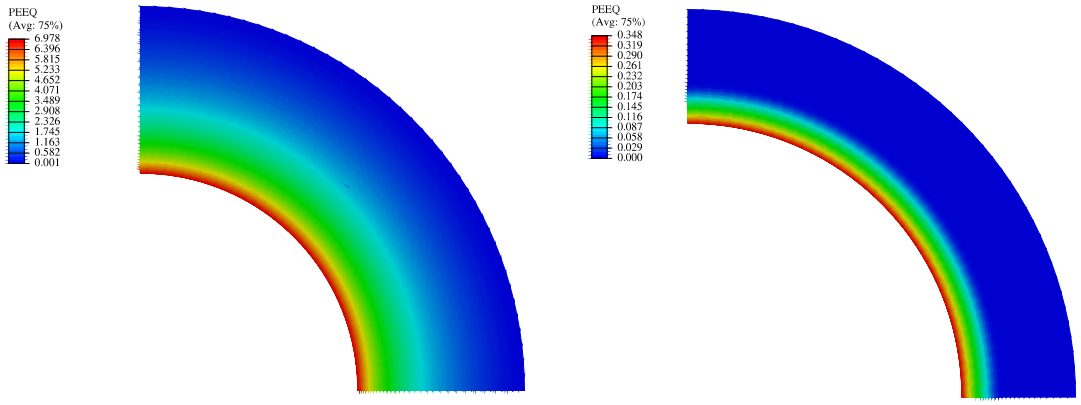

(a) Plastic strain distribution in inner layer (b) Plastic strain distribution in outer layer

Fig. 8. Plastic strain distribution of double-layer tube in plastic limit due to failure of inner layer.

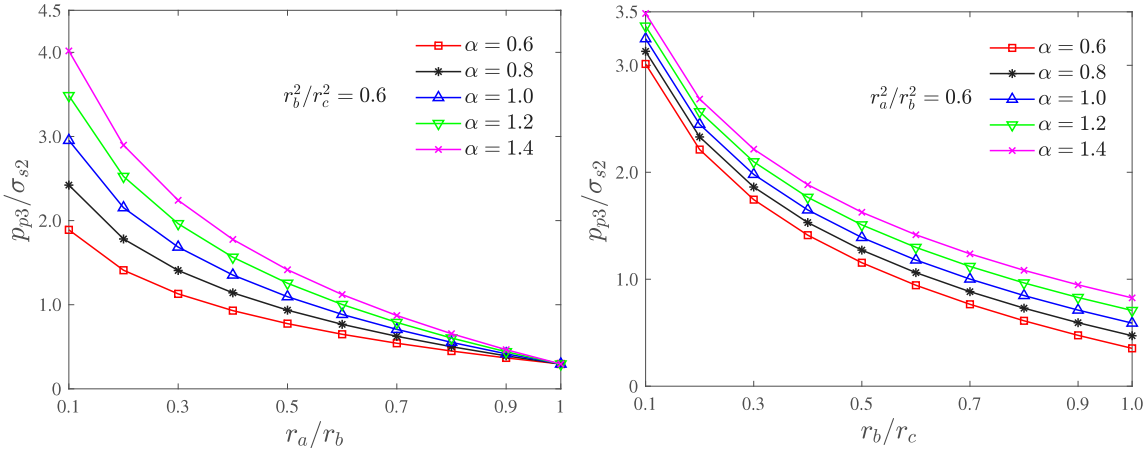

(a) Curves of $p_{p3}/\sigma_{s2} - r_a/r_b$ under different α (b) Curves of $p_{p3}/\sigma_{s2} - r_a/r_b$ under different α

Fig. 9. Variation of p_{p3} with respect to different geometric dimensions.

3.2.3. The plastic failure of inner and outer layers at the same time

In this part, we consider the plastic limit of tube due to the failure of inner and outer layers at the same time. In this situation, the elastoplastic radius of the inner layer is $r_i = r_b$ and the elastoplastic radius of the outer layer is $r_o = r_c$. Then, the following conditions should be satisfied:

$$\alpha = \beta k_2^{-1} - \frac{1}{2}(1-\nu_1)\ln k_2 \tag{52}$$

By integrating Eqs. (39) and (40), the plastic limit of double-layer tube is:

$$p_{p3} = -\frac{1}{\sqrt{3}}\sigma_{s2}\ln(k_1^{\alpha}k_2) \tag{53}$$

It is considered that the yield limit of the inner and outer layers is the same $\sigma_{s1} = \sigma_{s2}$, then the plastic limit of the double-layer tube composed of same material can be obtained by Eq. (53). The reduced result $p_{p3} = -[\sigma_{s2}\ln(k_1k_2)]/\sqrt{3}$ is in consistent with the that in [18] of single layer tube, indicating that the result of Eq. (53) is general.

As shown in Fig. 9, we can easily observe that the plastic limit p_{p3} increases with the parameter α. It is indicated that yield limit of inner layer is more important to plastic limit of double-layer tube. However, we can see p_{p3} decreases as the thickness of the inner and outer layer decreases.

3.3. Discussion on plastic failure modes

It is found that the relationship between α and the k_2 will affect the plastic failure mode of the double-layer tube, which may be the plastic failure of the inner layer, the plastic failure of the outer layer, or the simultaneous failure of the inner and outer layers.

Fig. 10 depicts the relationship between the yield strength ratio and the geometric size of the double-layer tube. From Fig. 10, we can find that there are three plastic failure modes of the double-layer tube. When the initial value locates on the upper side of the curve, the outer layer plastic failure will firstly occur. When the initial value locates on the curve, the inner and outer layers plastic failure will occur simultaneously, When the initial value locates on the lower side of the curve, the inner layer plastic failure will firstly occur.

4. Shakedown analysis of double-layer tube

In this section, we will consider the cyclic loading case. In order to prevent the incremental collapse and fatigue failure, the structure should undergo plastic deformation in the initial finite cycles, and the response of the structure is pure elastic in the subsequent cycles. Therefore, the main task is to determining the critical shakedown load of double layer tube.

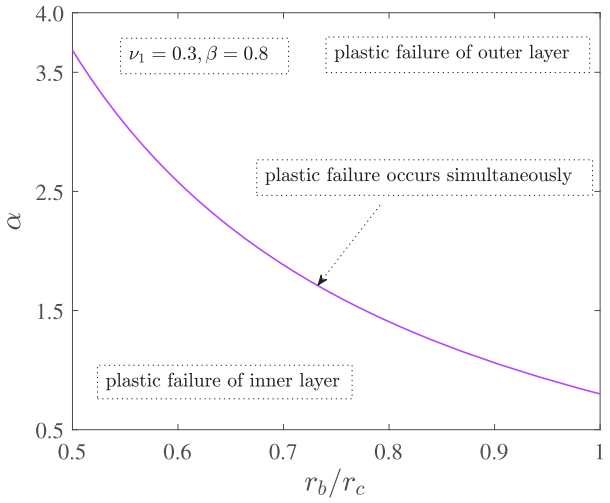

Fig. 10. Variation of α with respect to different geometric dimensions and different failure modes.

4.1. The relationship between shakedown limit and plastic limit for different failure mechanism

According to previous research of hollow sphere under cyclic load [19], the structure might fail due to fatigue or excessive deformation at the first cycle if the load amplitude is too large. Therefore, it is also necessary to determine the failure mechanism of double layer tube depending on the geometric dimension and load amplitude.

For a single layer tube, if shakedown limit less than plastic limit, the following condition is obtained considering Eqs. (14) and (22):

$$\sigma_s(1-k) + \frac{1}{2}\sigma_s \ln k < 0 \tag{54}$$

which is satisfied if:

$$0 < k < 0.203 \tag{55}$$

Therefore, if the dimension condition (55) is fulfilled, the tube will fail due to fatigue. Otherwise, the excessive deformation of the structure will lead to the fracture of tube at the first cycle. It can be seen the size of the shakedown limit and plastic limit is related to the volume fraction k.

Therefore, the shakedown limit of double-layer tube can be discussed in four cases by considering different volume fractions of inner layer k_1 and outer layer k_2. Four cases (1) $0 < k_1 < 0.203$ and $0 < k_2 < 0.203$, (2) $0 < k_1 < 0.203$ and $0.203 < k_2 < 1$, (3) $0.203 < k_1 < 1$ and $0 < k_2 < 0.203$, (4) $0.203 < k_1 < 1$ and $0.203 < k_2 < 1$ need to be discussed. Case 2 and case 3 are similar, so the computation of long-term strength of case 3 is provided in Appendix in order to avoid repetition.

4.2. The shakedown limit analysis for $0 < k_1 < 0.203$ and $0 < k_2 < 0.203$

In this part, both the inner and outer layers will fail due to fatigue collapse. If $q = \sigma_{s2}(1-k_2)$ which is shakedown limit of outer layer, the outer layer will be in a critical state. Using Eq. (40), its critical elastoplastic radius is $r_o = \xi r_c$, where coefficient ξ can be obtain as:

$$\xi^2 - 2ln\xi + lnk_2 - 2k_2 + 1 = 0 \tag{56}$$

Similarly, the critical elastic–plastic radius of inner layer is $r_i = \eta r_b$, where coefficient η is given by:

$$\eta^2 - 2ln\eta + lnk_1 - 2k_1 + 1 = 0 \tag{57}$$

4.2.1. The fracture occurs firstly in the inner layer due to fatigue

If the inner layer is firstly fail due to fatigue, its elastoplastic radius exceeds the critical value. In other words, if $r_o = \xi r_c$, then $r_i > \eta r_b$. Using Eq. (43), the following equation can be given:

$$\alpha < (1-\nu_1)(1-k_2)\eta^{-2} + \frac{1}{2}\beta\xi^2\eta^{-2}k_2^{-1}[1+\nu_2+(1-\nu_2)\xi^2] \tag{58}$$

The elastoplastic radius of the outer layer can be calculated by the use of the critical state of the inner layer. Taking $r_i = \eta r_b$ and Eq. (43) into account, we can obtain $r_o = \lambda_3 r_c$, in which the coefficient λ_3 is:

$$(1-\nu_1)(1-\lambda_3^2+\ln\lambda_3^2k_2^{-1}) + \beta\lambda_3^2k_2^{-1}[1+\nu_2+(1-\nu_2)\lambda_3^2] - 2\alpha\eta^2 = 0 \tag{59}$$

By substituting the elastoplastic radius $r_i = \eta r_b$ of the inner layer and the elastoplastic radius $r_o = \lambda_3 r_c$ of the outer layer into Eqs. (39) and (40), the shakedown limit of the double-layer tube in this case can be deduced as:

$$p_{sd1} = \frac{1}{\sqrt{3}}\sigma_{s2}[1-\lambda_3^2+2\alpha(1-k_1)+\ln\lambda_3^2k_2^{-1}] \tag{60}$$

Figs. 11 and 12 illustrate the comparison between analytical results and numerical ones of the shakedown limit for $r_a^2/r_b^2 = 0.16, r_b^2/r_c^2 = 0.16$. The elastic constants are $\alpha = 1.3, \nu_1 = \nu_2 = 0.3$ and $\beta = 1$. Since the fatigue failure occurs firstly in the inner layer, the accumulative equivalent plastic strain of the inner layer continuously increases, while the plastic strain of the outer layer tends to remain constant.

4.2.2. The fracture occurs firstly in the outer layer due to fatigue

If the outer layer is firstly fail due to fatigue, the corresponding elastoplastic radius firstly exceeds the critical value. In other words, if $r_o = \xi r_c$, then $r_i < \eta r_b$. Similar to the fatigue failure of inner layer, we can deduce:

$$\alpha > (1-\nu_1)(1-k_2)\eta^{-2} + \frac{1}{2}\beta\xi^2\eta^{-2}k_2^{-1}[1+\nu_2+(1-\nu_2)\xi^2] \tag{61}$$

The following elastoplastic radius corresponding to the inner layer is derived based on the critical state of the outer layer. If $r_o = \xi r_c$, we can get $r_i = \lambda_4 r_b$ by Eq. (43), in which the coefficient λ_4 is given by:

$$(1-\nu_1)(1-\xi^2+\ln\xi^2k_2^{-1}) + \beta\xi^2k_2^{-1}[1+\nu_2+(1-\nu_2)\xi^2] - 2\alpha\lambda_4^2 = 0 \tag{62}$$

Substituting $r_i = \lambda_4 r_b$ and $r_o = \xi r_c$ into Eqs. (39) and (40), and the shakedown limit of the double-layer tube is computed as:

$$p_{sd2} = \frac{1}{\sqrt{3}}\sigma_{s2}[\alpha(1-\lambda_4^2)+2(1-k_2)+\ln\lambda_4^{2\alpha}k_1^{-\alpha}] \tag{63}$$

4.2.3. Simultaneous fatigue failure of inner and outer layers

If the inner and outer layer reach the shakedown limit at the same time, that is, if $r_o = \xi r_c$, then $r_i = \eta r_b$. We can still have:

$$\alpha = (1-\nu_1)(1-k_2)\eta^{-2} + \frac{1}{2}\beta\xi^2\eta^{-2}k_2^{-1}[1+\nu_2+(1-\nu_2)\xi^2] \tag{64}$$

By obtaining the elastoplastic radius $r_i = \eta r_b$ and $r_o = \xi r_c$, we substitute them into Eqs. (39) and (40), and the shakedown limit of the double-layer tube can be written as:

$$p_{sd3} = \frac{2}{\sqrt{3}}\sigma_{s2}[1-k_2+\alpha(1-k_1)] \tag{65}$$

Fig. 13 illustrates the shakedown limit p_{sd3} with respect to different geometric dimensions of inner and outer layers (left and right subfigures). It can be founded that when the thickness of the inner or outer layer decreases, the shakedown limit of both the two layers also decreases. However, the larger the yield limit ratio *alpha* of double-layer tube is, the greater the shakedown limit will be, which indicates that the yield limit of the inner layer has a greater influence on the shakedown limit of the double-layer tube.

It can be found from Fig. 14 that the double-layer tube has higher long-term strength than the single-layer tube having the same thickness and yield stress of metal solid. If the yield stress of the double-layer tube is 60% of that of the single-layer tube, the bearing capacity can also be

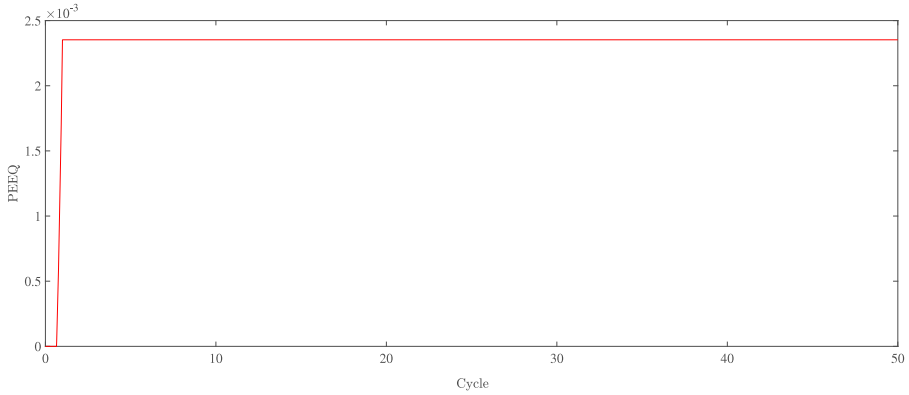

Fig. 11. Accumulative equivalent plastic strain(PEEQ) of outer layer does not increase after first loading.

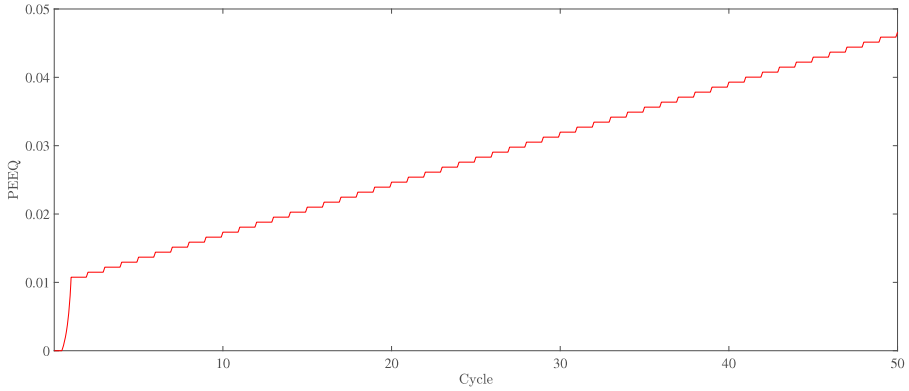

Fig. 12. Accumulative equivalent plastic strain(PEEQ) of the inner layer is continuously increasing under cyclic loading.

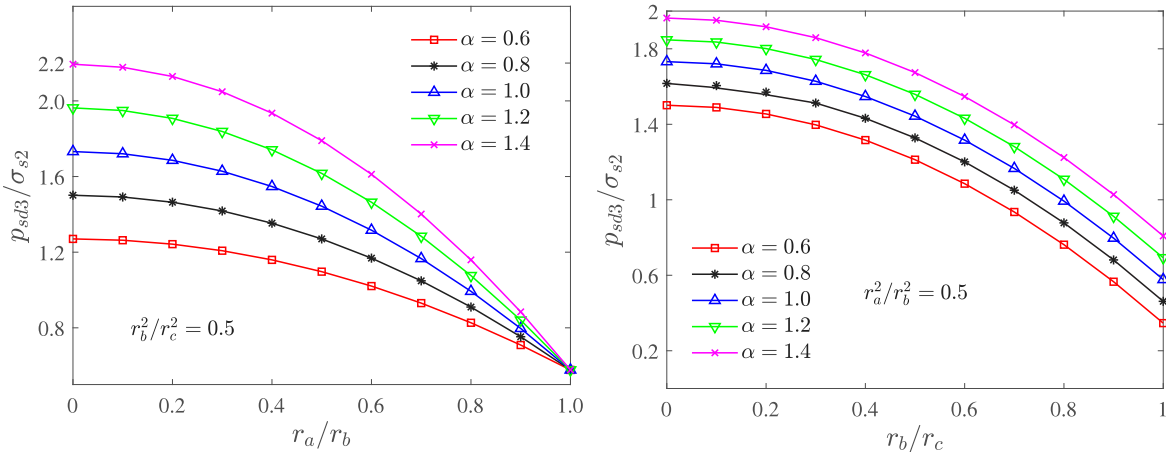

(a) Curves of $p_{sd3}/\sigma_{s2} - r_a/r_b$ under different α (b) Curves of $p_{sd3}/\sigma_{s2} - r_b/r_c$ under different α

Fig. 13. Variation of p_{sd3} with respect to different geometric dimensions.

compensated by increasing the thickness. However, with the infinite increase of thickness, the shakedown limit finally tends to be constant. If we keep the thickness of the double-layer tube constant, it can be found that the intermediate radius r_b will also affect the shakedown limit of the double-layer tube. The specific value of the intermediate radius can be determined according to Eq. (36). Compared with Fig. 6, it can be found that when the inner and outer layers fatigue failure occurs at the same time, the shakedown limit of the double cylinder is twice the elastic limit, as that described in [19] for ductile porous materials.

4.3. *The shakedown limit analysis for* $0 < k_1 < 0.203$ *and* $0.203 < k_2 < 1$

In this case, the situation is that the shakedown limit of inner layer is less than the plastic limit and shakedown limit of outer layer is more than plastic limit. Considering the effect of total contact pressure q on outer layer, if $q = -(\sigma_{s2} \ln k_2)/2$, the outer layer will be in a critical state. The critical elastic–plastic radius is $r_o = r_c$.

4.3.1. *The fracture occurs firstly in the inner layer due to fatigue*

If the inner layer is firstly failed due to fatigue, the elastic–plastic radius firstly exceeds the critical radius. In other words, if $r_o = r_c$, then

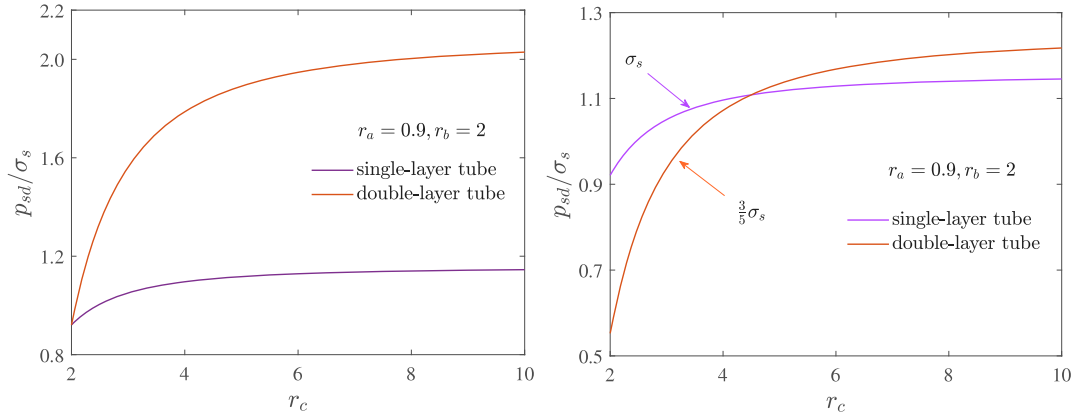

(a) Curves of $p_{sd}/\sigma_s - r_c$ under indentical yield strength between single-layer tube and double-layer tube

(b) Curves of $p_{sd}/\sigma_s - r_c$ under different yield strength between single-layer tube and double-layer tube

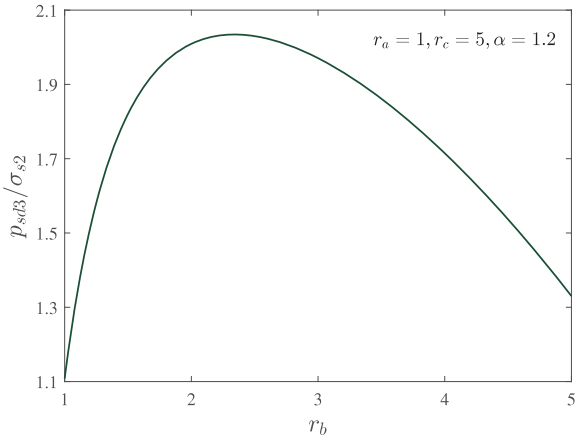

(c) Curve of $p_{sd3}/\sigma_{s2} - r_b$ with repect to ratio $\alpha = \sigma_{s1}/\sigma_{s2}$.

Fig. 14. Comparison of long-term strength between single-layer tube and double-layer tube under cyclic loading.

$r_i > \eta r_b$. One has:

$$\alpha < \beta\eta^{-2}k_2^{-1} + \frac{1}{2}(1-\nu_1)\eta^{-2}\ln k_2^{-1} \tag{66}$$

The elastic–plastic radius of the outer layer is calculated based on the critical state of the inner layer. If $r_i = \eta r_b$, then we can get $r_o = \lambda_5 r_c$ by Eq. (43), in which the coefficient λ_5 can be obtain as:

$$(1-\nu_1)(1-\lambda_5^2 + \ln\lambda_5^2 k_2^{-1}) + \beta\lambda_5^2 k_2^{-1}[1+\nu_2+(1-\nu_2)\lambda_5^2] - 2\alpha\eta^2 = 0 \tag{67}$$

Substituting the elastic–plastic radius $r_i = \eta r_b$ and the elastic–plastic radius $r_o = \lambda_5 r_c$ into Eqs. (39) and (40), the shakedown limit of the double-layer tube in this case can be obtained:

$$p_{sd1} = \frac{1}{2}\sigma_{s2}[1-\lambda_5^2 + 2\alpha(1-k_1) + \ln\lambda_5^2 k_2^{-1}] \tag{68}$$

4.3.2. Plastic failure occurs firstly in the outer layer

If the tube is destroyed due to the excessive deformation of outer layer, the elastoplastic radius firstly exceeds the critical radius. If $r_o = r_c$, then $r_i < \eta r_b$. Then one has:

$$\alpha > \beta\eta^{-2}k_2^{-1} + \frac{1}{2}(1-\nu_1)\eta^{-2}\ln k_2^{-1} \tag{69}$$

The elastoplastic radius of the inner layer is calculated by considering $r_o = r_c$, then we can get $r_i = \lambda_6 r_b$ with Eq. (43), where the coefficient λ_6 is given by:

$$(1-\nu_1)k_2\ln k_2 + 2\alpha\lambda_6^2 k_2 - 2\beta = 0 \tag{70}$$

By substituting $r_i = \lambda_6 r_b$ of the inner layer and $r_o = r_c$ of the outer layer into Eqs. (39) and (40), the shakedown limit of the double-layer tube is:

$$p_{sd2} = \frac{1}{2}\sigma_{s2}[\alpha(1-\lambda_6^2) + \ln\lambda_6^{2\alpha}k_1^{-\alpha}k_2^{-1}] \tag{71}$$

4.3.3. Simultaneous failure of inner layer and outer layer

If the outer layer reaches the plastic limit and the inner layer reaches the shakedown limit simultaneously, the critical elastoplastic radii will be both reached. if $r_o = r_c$, then $r_i = \eta r_b$. We can still get:

$$\alpha = \beta\eta^{-2}k_2^{-1} + \frac{1}{2}(1-\nu_1)\eta^{-2}\ln k_2^{-1} \tag{72}$$

By substituting $r_i = \eta r_b$ and $r_o = r_c$ into Eqs. (39) and (40), the shakedown limit of the double-layer tube in this case can be obtained:

$$p_{sd3} = \frac{1}{2}\sigma_{s2}[2\alpha(1-k_1) - \ln k_2] \tag{73}$$

4.4. The shakedown limit analysis for $0.203 < k_1 < 1$ and $0.203 < k_2 < 1$

For this case of double-layer tube, its shakedown limit is greater than the plastic limit for both inner and outer layers. And the maximum value of cyclic load should not exceed the plastic limit.

Through the previous discussion of the plastic limit, it is known that if the relationship between α and k_2 satisfies:

$$\alpha < \beta k_2^{-1} - \frac{1}{2}(1-\nu_1)\ln k_2 \tag{74}$$

the shakedown limit of the double-layer tube is:

$$p_{sd1} = \frac{1}{\sqrt{3}}\sigma_{s2}[1 - \lambda_1^2 + \ln(\lambda_1^2 k_1^{-\alpha} k_2^{-1})] \tag{75}$$

If the relationship between α and k_2 satisfies:

$$\alpha > \beta k_2^{-1} - \frac{1}{2}(1 - \nu_1)\ln k_2 \tag{76}$$

the shakedown limit of the double-layer tube is:

$$p_{sd2} = \frac{1}{\sqrt{3}}\sigma_{s2}[\alpha - \alpha\lambda_2^2 + \ln(\lambda_2^{2\alpha} k_1^{-\alpha} k_2^{-1})] \tag{77}$$

If the relationship between α and k_2 satisfies:

$$\alpha = \beta k_2^{-1} - \frac{1}{2}(1 - \nu_1)\ln k_2 \tag{78}$$

the shakedown limit of the double-layer tube is:

$$p_{sd3} = -\frac{1}{\sqrt{3}}\sigma_{s2}\ln(k_1^{\alpha} k_2) \tag{79}$$

Consequently, it can be concluded that the long-term strength of double-layer tube can be determined depending on the ratio of yield stress and volume fraction of inner and outer layers, but not on the elastic properties.

5. Conclusion

In this study, by the use of the displacement continuity condition, we derive the elastic, plastic and shakedown limits of the double-layer tube when the inner and outer layers composed of different materials in the framework of limit and shakedown analysis. The elastic constants and geometric dimensions of the inner and outer layers are reasonably considered. It is found that the intermediate radius has an important influence on the elastic limit. An optimal intermediate radius of the double-layer tube is can increase the elastic limit.

Especially, the effects of different geometric sizes and material properties (elastic modulus, Poisson's ratio and yield stress) of double layers on the plastic limit under monotonic load and shakedown limit under cyclic load have been fully discussed. The result shows that the bearing capacity of the double-layer tube under monotonic loading will reach the maximum value, when the inner and outer layers reach the elastic limit or the plastic limit at the same time. The computation of long-term strength are divided into 4 different cases by considering the different volume fraction of inner and outer layers. The two-layer structure may fail due to different mechanism (fatigue and excessive deformation at first cycle) of inner or outer layers. Interestingly, Only when they reach the shakedown limit at the same time, the shakedown limit of the double-layer tube will reach the maximum value. At this time, like the single-layer tube, the shakedown limit of the double-layer tube is also twice of the elastic limit. Compared with the single-layer tube, it is found that the bearing capacity of the double-layer one has been significantly improved by applying appropriate geometric dimension and material in the fabrication in short-term and long-term.

CRediT authorship contribution statement

Jiajiang Du: Data curation, Writing – original draft. **Jin Zhang:** Methodology, Writing – reviewing and editing. **Yanhui Liu:** Software, Writing – reviewing and editing. **Chong Shi:** Conceptualization, Supervision. **Xiusong Shi:** Writing – reviewing and editing, Supervision.

Declaration of competing interest

The authors declare that they have no known competing financial interests or personal relationships that could have appeared to influence the work reported in this paper.

Data availability

Data will be made available on request.

Acknowledgments

The authors would like to thank the National Natural Science Foundation of China (Grant No. 11902111) and the Funds for the Disciplinary Development, China (Research Starting Funds for High-level Talents: Grant No. 522020212) for the support.

Appendix. Shakedown limit analysis of double-layer tube for $0.203 < k_1 < 1$ and $0 < k_2 < 0.203$

In this part, the shakedown limit of inner layer is considered larger than the plastic limit, and the shakedown limit of outer layer is less than plastic limit. Considering the effect of total contact pressure q on outer layer, if $q = \sigma_{s2}(1 - k_2)$, the outer layer will be in a critical state, where critical elastic–plastic radius is $r_o = \xi r_c$.

A.1. The fracture occurs firstly in the inner layer due to excessive plastic deformation at first cycle

If the inner layer is destroyed firstly due to excessive plastic deformation, the elastoplastic radius firstly exceeds the critical value. In other words, if $r_o = \xi r_c$, then $r_i > r_b$. We can still get:

$$\alpha < (1 - \nu_1)(1 - k_2) + \frac{1}{2}\beta\xi^2 k_2^{-1}[1 + \nu_2 + (1 - \nu_2)\xi^2] \tag{80}$$

The elastoplastic radius of the outer layer is calculated by the critical state of the inner layer. If $r_i = r_b$, then we can get $r_o = \lambda_7 r_c$ through Eq. (43), in which the coefficient λ_7 is given by:

$$(1 - \nu_1)(1 - \lambda_7^2 + \ln\lambda_7^2 k_2^{-1}) + \beta\lambda_7^2 k_2^{-1}[1 + \nu_2 + (1 - \nu_2)\lambda_7^2] - 2\alpha = 0 \tag{81}$$

Substituting them into the stress continuity condition Eqs. (39) and (40), the shakedown limit of the double-layer tube is:

$$p_{sd1} = \frac{1}{2}\sigma_{s2}[1 - \lambda_7^2 + \ln(\lambda_7^2 k_1^{-\alpha} k_2^{-1})] \tag{82}$$

A.2. The fracture occurs firstly in the outer layer due to fatigue

If the fatigue collapse of outer layer is firstly arrived, the elastoplastic radius will exceeds the critical value. That is, if $r_o = \xi r_c$, then $r_i < r_b$. One has the following relation:

$$\alpha > (1 - \nu_1)(1 - k_2) + \frac{1}{2}\beta\xi^2 k_2^{-1}[1 + \nu_2 + (1 - \nu_2)\xi^2] \tag{83}$$

The elastoplastic radius of the inner layer is calculated based on the critical state of the outer layer. If $r_o = \xi r_c$, then we can get $r_i = \lambda_8 r_b$ by using Eq. (43), where the coefficient of λ_8 is given by:

$$(1 - \nu_1)[1 - \xi^2 + \ln(\xi^2 k_2^{-1})] + \beta\xi^2 k_2^{-1}[1 + \nu_2 + (1 - \nu_2)\xi^2] - 2\alpha\lambda_8^2 = 0 \tag{84}$$

After calculating the maximum elastic–plastic radius of the outer layer and the corresponding elastoplastic radius of the inner layer, the maximum value of elastoplastic radius of the outer layer and the corresponding elastic–plastic radius of the inner layer are substituted into the stress continuity condition Eqs. (39) and (40), and the shakedown limit of the double-layer tube can be obtained:

$$p_{sd2} = \frac{1}{2}\sigma_{s2}[\alpha(1 - \lambda_8^2) + 2(1 - k_2) + \ln(\lambda_8^{2\alpha} k_1^{-\alpha})] \tag{85}$$

A.3. Simultaneous failure of inner layer (fatigue) and outer layer (excessive deformation)

If the outer layer reaches the shakedown limit and the inner layer reaches the plastic limit simultaneously, that is $r_o = \xi r_c$, then $r_i = r_b$. The following equation can be obtained:

$$\alpha = (1-\nu_1)(1-k_2) + \frac{1}{2}\beta\xi^2 k_2^{-1}[1+\nu_2+(1-\nu_2)\xi^2] \tag{86}$$

After obtaining the elastoplastic radii of the outer and inner layers, it is substituted into the stress continuity condition Eqs. (39) and (40). The shakedown limit of the double-layer tube is:

$$p_{sd3} = \frac{1}{2}\sigma_{s2}[2(1-k_2) - \alpha \ln k_2] \tag{87}$$

References

[1] H.F. Abdalla, A novel methodology for determining the elastic shakedown limit loads via computing the plastic work dissipation, Int. J. Press. Vessels Pip. 191 (2021) 104327.

[2] H. Peng, Y. Liu, H. Chen, Shakedown analysis of elastic-plastic structures considering the effect of temperature on yield strength: theory, method and applications, Eur. J. Mech. A Solids 73 (2019) 318–330.

[3] R. Singh, P. Singh, A. Kumar, Unusual extension–torsion–inflation couplings in pressurized thin circular tubes with helical anisotropy, Math. Mech. Solids 24 (9) (2019) 2694–2712.

[4] H. Darijani, M. Kargarnovin, R. Naghdabadi, Design of thick-walled cylindrical vessels under internal pressure based on elasto-plastic approach, Mater. Des. 30 (9) (2009) 3537–3544.

[5] N.-H. Kim, C.-S. Oh, Y.-J. Kim, J.-S. Kim, D.W. Jerng, P.J. Budden, Limit loads and fracture mechanics parameters for thick-walled pipes, Int. J. Press. Vessels Pip. 88 (10) (2011) 403–414.

[6] R. Sharma, A. Aggarwal, S. Sharma, Collapse pressure analysis in torsion of a functionally graded thick-walled circular cylinder under external pressure, Procedia Eng. 86 (2014) 738–747.

[7] X. Guojun, W. Jianhua, A rigorous characteristic line theory for axisymmetric problems and its application in circular excavations, Acta Geotech. 15 (2) (2020) 439–453.

[8] X. Ni, X. Liu, Y. Liu, Calculation of ultimate loads and stable loads of strength-differential thick cylinders by the twin shear strength theory, in: 4th International Symposium on Test and Measurement, Shanghai, 2001, pp. 1102–1104.

[9] A. Benslimane, C. Medjdoub, M. Methia, M.A. Khadimallah, D. Hammiche, Investigation of displacement and stress fields in pressurized thick-walled FGM cylinder under uniform magnetic field, Mater. Today: Proc. 36 (2021) 101–106.

[10] S. Saeedi, M. Kholdi, A. Loghman, H. Ashrafi, M. Arefi, Thermo-elasto-plastic analysis of thick-walled cylinder made of functionally graded materials using successive approximation method, Int. J. Press. Vessels Pip. 194 (2021) 104481.

[11] V. Shlyannikov, Fatigue shape analysis for internal surface flaw in a pressurized hollow cylinder, Int. J. Press. Vessels Pip. 77 (5) (2000) 227–234.

[12] Y. Cao, T. Tamura, H. Kawai, Investigation of wall pressures and surface flow patterns on a wall-mounted square cylinder using very high-resolution Cartesian mesh, J. Wind Eng. Ind. Aerodyn. 188 (2019) 1–18.

[13] J. Zhang, J. Shao, Q. Zhu, G. De Saxcé, A variational-based homogenization model for plastic shakedown analysis of porous materials with a large range of porosity, Int. J. Mech. Sci. 199 (2021) 106429.

[14] Q.-Y. Zhang, Computation for the torsion of a thick-walled tube with fillets using tapered section assumption, Int. J. Press. Vessels Pip. 77 (8) (2000) 473–478.

[15] M.Z. Nejad, P. Fatehi, Exact elasto-plastic analysis of rotating thick-walled cylindrical pressure vessels made of functionally graded materials, Internat. J. Engrg. Sci. 86 (2015) 26–43.

[16] M. Takla, Instability and axisymmetric bifurcation of elastic-plastic thick-walled cylindrical pressure vessels, Int. J. Press. Vessels Pip. 159 (2018) 73–83.

[17] Q. Zhu, J. Zhao, C. Zhang, Y. Li, S. Wang, Elastic–brittle–plastic analysis of double-layered combined thick-walled cylinder under internal pressure, J. Press. Vessel Technol. 138 (1) (2016).

[18] D. Weichert, G. Maier, Inelastic Behaviour of Structures under Variable Repeated Loads: Direct Analysis Methods, Vol. 432, Springer, 2014.

[19] J. Zhang, W. Shen, A. Oueslati, G. De Saxcé, Shakedown of porous materials, Int. J. Plast. 95 (2017) 123–141.

[20] A. Yavari, A. Goriely, The twist-fit problem: finite torsional and shear eigenstrains in nonlinear elastic solids, Proc. R. Soc. A 471 (2183) (2015) 20150596.

[21] N. Cohen, Stacked dielectric tubes with electromechanically controlled radii, Int. J. Solids Struct. 108 (2017) 40–48.

[22] N. Emuna, N. Cohen, Inflation-induced twist in geometrically incompatible isotropic tubes, J. Appl. Mech. 88 (3) (2021).

[23] N. Emuna, N. Cohen, Inversion and perversion in twist incompatible isotropic tubes, Extreme Mech. Lett. 46 (2021) 101303.

[24] N. Emuna, D. Durban, Stability analysis of arteries under torsion, J. Biomech. Eng. 142 (6) (2020) 061011.

[25] H. Hui, P. Li, Plastic limit load analysis for steam generator tubes with local wall-thinning, Nucl. Eng. Des. 240 (10) (2010) 2512–2520.

[26] S. Poonaya, U. Teeboonma, C. Thinvongpituk, Plastic collapse analysis of thin-walled circular tubes subjected to bending, Thin-Walled Struct. 47 (6–7) (2009) 637–645.

[27] J. Zhang, W. Liu, Q. Zhu, J. Shao, A novel elastic–plastic damage model for rock materials considering micro-structural degradation due to cyclic fatigue, Int. J. Plast. (2022) 103496.

[28] A. Ampatzis, V. Psomiadis, E. Efthymiou, Plastic collapse of hardening spatial aluminium frames: A novel shakedown-based approach, Eng. Struct. 151 (2017) 724–744.

[29] D. Floros, A. Ekberg, K. Runesson, A numerical investigation of elastoplastic deformation of cracks in tubular specimens subjected to combined torsional and axial loading, Int. J. Fatigue 91 (2016) 171–182.

[30] J. Zhang, A. Oueslati, W.Q. Shen, G. De Saxcé, Shakedown of porous material with Drucker-Prager dilatant matrix under general cyclic loadings, Compos. Struct. 220 (2019) 566–579.

[31] E. Melan, Theory statisch unbestimmter systeme aus ideal plastischen baustoff, Sitzber. Akad. Wiss. (1936) 145–195.

[32] W. Koiter, General theorems for elastic-plastic solids, in: Progress in Solid Mechanics, Vol. 1, 1960.

[33] M. Abdel-Karim, Shakedown of complex structures according to various hardening rules, Int. J. Press. Vessels Pip. 82 (6) (2005) 427–458.

[34] R. Gumruk, A numerical investigation of dynamic plastic buckling behaviour of thin-walled cylindrical structures with several geometries, Thin-Walled Struct. 85 (2014).

[35] H.F. Abdalla, M.M. Megahed, M.Y. Younan, A simplified technique for shakedown limit load determination, Nucl. Eng. Des. 237 (12–13) (2007) 1231–1240.

[36] H.F. Abdalla, M.M. Megahed, M.Y. Younan, A simplified technique for shake-down limit load determination of a large square plate with a small central hole under cyclic biaxial loading, Nucl. Eng. Des. 241 (3) (2011) 657–665.

[37] X. Chen, X. Chen, D. Yu, B. Gao, Recent progresses in experimental investigation and finite element analysis of ratcheting in pressurized piping, Int. J. Press. Vessels Pip. 101 (2013) 113–142.